BMB
Reports

BMB Rep. 2024; 57(9): 417-423
www.bmbreports.org

Glucose-dependent insulinotropic polypeptide (GIP) alleviates ferroptosis in aging-induced brain damage through the Epac/Rap1 signaling pathway

Jiwon Ko[2,#], Soyoung Jang[1,#], Soyeon Jang[2], Song Park[6,7], Junkoo Yi[5], Dong Kyu Choi[1], Seonggon Kim[4], Myoung Ok Kim[3], Su-Geun Lim[2,] & Zae Young Ryoo[1,*]*

[1]School of Life Science and Biotechnology, College of Natural Sciences, BK21 FOUR KNU Creative BioResearch Group, Kyungpook National University, Daegu 41566, [2]Institute of Life Science and Biotechnology, Kyungpook National University, Daegu 41566, [3]Department of Animal Science and Biotechnology, Kyungpook National University, Sangju 37224, [4]Preclinical Research Center, Daegu-Gyeongbuk Medical Innovation Foundation, Daegu 41061, [5]School of Animal Life Convergence Science, Hankyong National University, Anseong 17579, [6]Division of Animal Science, Gyeongsang National University, Jinju 52828, [7]Institute of Agriculture and Life Science (IALS), Gyeongsang National University, Jinju 52828, Korea

Glucose-dependent insulinotropic polypeptide (GIP), a 42-amino-acid hormone, exerts multifaceted effects in physiology, most notably in metabolism, obesity, and inflammation. Its significance extends to neuroprotection, promoting neuronal proliferation, maintaining physiological homeostasis, and inhibiting cell death, all of which play a crucial role in the context of neurodegenerative diseases. Through intricate signaling pathways involving its cognate receptor (GIPR), a member of the G protein-coupled receptors, GIP maintains cellular homeostasis and regulates a defense system against ferroptosis, an essential process in aging. Our study, utilizing GIP-overexpressing mice and *in vitro* cell model, elucidates the pivotal role of GIP in preserving neuronal integrity and combating age-related damage, primarily through the Epac/Rap1 pathway. These findings shed light on the potential of GIP as a therapeutic target for the pathogenesis of ferroptosis in neurodegenerative diseases and aging. [BMB Reports 2024; 57(9): 417-423]

INTRODUCTION

Glucose-dependent insulinotropic polypeptide (GIP) is a 42-amino-acid polypeptide initially discovered in endocrine K cells of the upper small intestine. While GIP's primary function as an incretin hormone involves inhibiting gastric secretion and enhancing insulin release during hyperglycemia, its signaling effects also reach to the brain (1). It also acts as a neurotrophic factor, promoting cell proliferation and protecting neurons by enhancing repair and blocking cell death. Through this, GIP demonstrates neuroprotective effects against various stressors implicated in neurodegenerative diseases like Alzheimer's and Parkinson's disease (2).

Ferroptosis, a form of programmed cell death instigated by iron-dependent lipid peroxidation through divalent iron or ester oxygenase, is critical in diverse physiological processes (3). Lipid peroxidation plays an important role in regulating the aging process, and extensive evidence suggests that lipid peroxidation increases with advancing age (4). Its impact on managing cellular homeostasis has become a central focus of contemporary aging research (5).

Neuronal complexity of the brain is a multifaceted process involving intricate cellular and molecular events (6). While neural interactions are largely associated with the activation of protein kinase A (PKA) by the second messenger cAMP, an alternative cAMP-dependent mechanism has emerged involving exchange protein directly activated by cAMP (Epac). Epac responds to fluctuations in cAMP concentrations, facilitating the activation of small Rap GTPases. Growing pieces of evidence suggest that Epac plays a significant role in cell physiology including integrin-mediated cell adhesion, vascular endothelial cell barrier formation, hormone gene expression, and mitogen-activated protein kinase (MAPK) signaling. Once, Epac functions as a cAMP-binding protein with guanine nucleotide exchange factor (GEF) activities for the small GTPase, Rap1 that modulate these cellular functions (7, 8). Thus, the Epac/Rap1 pathway is valuable for cell growth, tissue damage, and homeostasis maintenance (9). Here, our findings unveil the exceptional role of GIP, acting through the Epac/Rap1 signaling pathway, in inhibiting ferroptotic cell death and maintaining homeostasis in the aging brain.

*Corresponding authors. Su-Geun Lim, Tel: +82-53-950-7361; Fax: +82-53-943-6925; E-mail: sugeun624@hanmail.net; Zae Young Ryoo, Tel: +82-53-950-7361; Fax: +82-53-943-6925; E-mail: jaewoong64@knu.ac.kr
#These authors contributed equally to this work.

https://doi.org/10.5483/BMBRep.2024-0067

**Received 7 May 2024, Revised 30 May 2024,
Accepted 24 July 2024, Published online 3 September 2024**

Keywords: Aging, Brain, Epac/Rap1, Ferroptosis, GIP

ISSN: 1976-670X (electronic edition)

RESULTS

GIP overexpressing cells exhibit enhanced cell proliferation

To examine the effect of the GIP gene in the brain, we transfected a GIP overexpressing vector with a neuron-specific enolase (NSE) promoter into the NB41A3 mouse neuroblastoma cell line. Then we confirmed that GIP mRNA expression increased approximately 140-fold (Fig. 1A) and a significant increase in GIP protein abundance was also seen (Fig. 1B). Next, using a CCK-8 assay, we showed that cell proliferation was enhanced after 24 h in the GIP overexpressing cells (Fig. 1C). Based on these data, the differences in cell cycle progression were further investigated using propidium iodide (PI) staining. Fluorescence-activated cell sorting (FACS) results showed that the proportion of cells in the G0/G1 phase ratio was reduced while that in the G2/M phase was significantly increased in NB41A3 cells overexpressing GIP (Fig. 1D, E). In addition, the mRNA expression level of Ki67 (Fig. 1F), a cell proliferation marker, was significantly increased in the GIP–overexpressing group, while those of p53 and p21 were decreased (Fig. 1G, H). These proteins regulate cell cycle arrest and death in various neurological diseases (10-12). Moreover, the mRNA expressions of cdc25a and three CDK-series proteins, which facilitate the cell cycle, were also elevated in the GIP overexpressing cells (Fig. 1I–L).

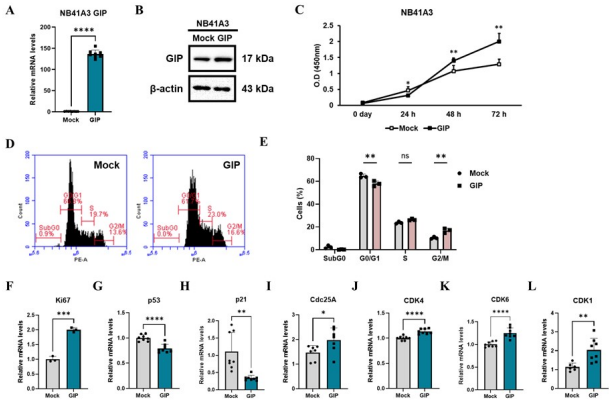

Fig. 1. GIP overexpression facilitates cell proliferation through a well-coordinated cell cycle progression in NB41A3 cells. The (A) mRNA expression and (B) protein levels of GIP were confirmed in mock and GIP overexpressing cells using qRT-PCR and Western blotting, respectively. (C) The rate of cell proliferation was analyzed daily using CCK-8 assays until 72 h to compare proliferation between the control (Mock) and GIP overexpressing cells. (D) NB41A3 cells were collected and stained with PI to monitor cell cycle profiles for a FACS analysis. (E) A bar graph displaying the percentage of cells in each cell phase. (F–L) Real-time qPCR was used to measure the relative mRNA expression levels of cell cycle markers. Data from three independent experiments are presented as means ± SEM, and t-tests were performed to assess statistical significance: *P < 0.05; **P < 0.01; ***P < 0.001; ****P < 0.0001.

GIP maintains cellular homeostasis and protects against ferroptotic cell death in NB41A3 cells by reducing lipid peroxidation, even in the absence of excessive inducers

The precision control of cell survival and death is crucial for maintaining homeostasis, facilitating cell-cell interactions, and regulating proliferation (13). In various neurodegenerative diseases, glutamate-induced oxidative stress causes a loss of cellular homeostasis and ultimately leads to neuronal cell death (14). To validate the adequate concentration of glutamate (Glu) needed to induce neuronal cytotoxicity in NB41A3 cells, we performed 24-hour glutamate treatments at increasing dosages on NB41A3, and cell viability was assessed (Fig. 2A). Cell viability continuously decreased, reaching about 50% with a 50 mM glutamate treatment. Though much higher glutamate concentrations were tested, NB41A3 cell viability was maintained even up to a glutamate concentration of 100 mM, with viability changing little above 150 mM. Therefore, we selected 100 mM glutamate as a treatment to trigger intracellular oxidative stress under conditions that could maximize the difference between mock and GIP cells. To further examine the effects of glutamate-induced ferroptosis, bright-

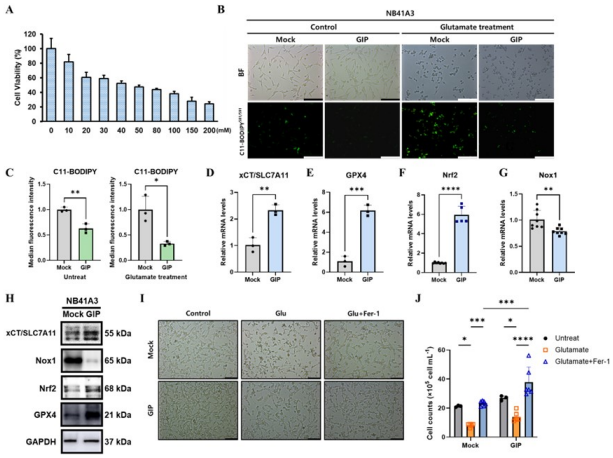

Fig. 2. GIP maintains cellular homeostasis by regulating lipid peroxidation in NB41A3 cells. (A) The viability of cells treated with glutamate at the indicated concentrations (x-axis) for 24 h was measured using CCK-8 assays. (B) Images of C11-BODIPY stained cells using a fluorescence microscope and bright-field images in the glutamate treatment or not. (C) The lipid peroxidation levels of cells treated with glutamate for 6 h and untreated cells (control) were measured using flow cytometry after C11-BODIPY staining. The median fluorescence intensity of flow cytometric results were quantified. (D-G) The relative mRNA levels of four ferroptosis marker genes. (H) Western blot data represent between mock and GIP overexpressing NB41A3 cells. (I-J) Bright-field images and quantification data indicate the mean of cell viability and recovery ability in the presence of Glu and Fer-1. All data from more than three independent experiments are presented as mean ± SEM, and t-tests were performed to assess statistical significance: *P < 0.05; **P < 0.01; ***P < 0.001; ****P < 0.0001.

field and C11-BODIPY$^{581/591}$ fluorescence images were taken (Fig. 2B). The C11-BODIPY$^{581/591}$ stain characteristically shifts from red to green fluorescence when lipids are oxidized, indicating lipid peroxidation (15). Therefore, we detected a significantly reduced level of green fluorescence intensity in the GIP overexpressing cells. A FACS analysis also showed that GIP exhibited low lipid peroxidation during the excessive glutamate treatment and even under normal untreated conditions (Fig. 2C). This indicates that intracellular homeostasis was much better preserved in the GIP overexpressing NB41A3 cells than in the mock cells, in general. In addition to the FACS results, previous studies using HT-22 overexpressing GIP cells also demonstrated the effectiveness of the GIP gene with or without glutamate treatment (16). Thus, to clarify the intracellular protective function of GIP itself, we measured the mRNA expression levels of ferroptosis-related markers without glutamate treatment. The relative mRNA expression levels of *xCT* (Fig. 2D),*GPX4* (Fig. 2E) (17), and Nrf2 (Fig. 2F) factors that suppress ferroptosis were elevated in the GIP overexpression group (18). In contrast, Nox1 (Fig. 2G), ferroptosis inducers, were significantly lower. The protein expression of relevant markers was also confirmed to be equally significant as the mRNA level (Fig. 2H). To affirm that GIP regulates glutamate-induced ferroptosis in NB41A3 cells, we observed a change in cell viability using a well-known ferroptosis inhibitor, Fer-1. We confirmed that cell recovery was significantly improved in GIP-overexpressing cell lines when treated with Fer-1 through cell morphology and quantification of cell counts (Fig. 2I, J). Therefore, NB41A3 neuronal cells overexpressing GIP run active homeostatic mechanisms even with no additional glutamate-induced oxidative stress.

GIP-overexpressing transgenic mice exhibit reduced ferroptosis

To determine the basal expression level of GIP *in vivo*, we first measured GIP levels in whole brains harvested from WT C57BL/6J mice at 13.5, 15.5, and 18.5 of the embryonic stage and at weeks 0, 1, and 10 of postnatal stage. In a western blot, the signal from the GIP protein bands was increased dramatically on day 15.5 of the embryonic stage (Fig. 3A). After that, expression remained high for the rest of the testing period without significant change until the 10-week stage. Given these findings, we assumed that GIP would play a more substantial role in adult mice. In Fig. 3B, the protein levels of GIP was confirmed in various tissues of wild-type (WT) mice at 11 weeks of age. As GIP is an incretin hormone (19), it was highly expressed in the gut (Fig. 3B). When the brain sections of 10-week-old wild-type mice were analyzed by region, the expression of GIP was exceptionally high in the cortex, hippocampus, and cerebellum and was lowest in the olfactory bulb of the mouse brain (Fig. 3C).

To prove the protective role of GIP in the mouse brain *in vivo*, we generated transgenic mice overexpressing GIP (GIP-TG mice) under the neuron-specific enolase (NSE) promoter using a vector that included a His-tagged stuffer gene (Fig. 3D). Genotyping was performed using RT-PCR to verify the successful generation of GIP-TG mice (Fig. 3E). In addition, we confirmed that the protein expression level of GIP was significantly higher in the whole brain of GIP-Tg mice compared to WT, thereby laying the foundation for establishing transgenic mice (Fig. 3F). Hematoxylin and eosin (H&E) staining was performed on sagittal sections spanning whole hemispheres 1-year-old mice, and the brain sections were imaged and measured (Fig. 3G). In control mice, several brain damage indicators were observed on the H&E-stained histological images that were absent in GIP-TG mice. In aging wild-type mouse brains, particularly in the cerebellum, hippocampus, and cerebral cortex, intracerebral hemorrhage around blood vessels (thin arrows in Fig. 3G) and a decrease in

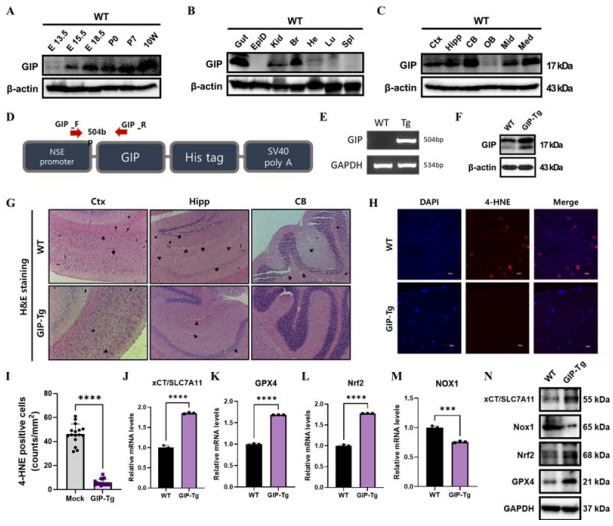

Fig. 3. GIP-overexpressing TG mice exhibit reduced aging-induced ferroptosis. (A) Western blotting analyses were performed to detect GIP protein expression in whole brain sections by period. (B) Proteins, including the gut, epididymis (EpiD), kidney (Kid), brain (Br), heart (He), lung (Lu), and spleen (Spl), in tissue samples from 11-week-old C57BL/6J WT mice were analyzed through western blotting. And (C) The cortex (Ctx), hippocampus (Hipp), cerebellum (CB), olfactory bulb (OB), midbrain (Mid), and medulla (Med) regions of WT mice were determined for GIP expression level. (D) A schematic showing the construction of the GIP-overexpression vector. (E) In TG mice, GIP-overexpression was confirmed using RT-PCR with primers targeting the transfected protein. (F) GIP level in mouse whole brain was analyzed in WT and GIP-Tg mice. (G) Light microscopy images of H&E-stained brain sagittal sections collected from 1-year-old mice (n = 3). (magnification: bar 100 μm). Thin arrows indicate intracerebral hemorrhages around blood vessels, and thick arrows indicate pyknotic nuclei. (H) Confocal microscopy images of cells stained with DAPI and immunostained for 4-HNE (red) in 1-year-old WT and GIP-TG mice, merged staining images are included on the right (scale bars represent 20 μm). (I) Quantification of 4-HNE positive cells (counts/mm^2). (J-M) mRNA levels of ferroptosis markers were assessed by qRT-PCR. (N) Protein levels of ferroptosis markers were evaluated by western blot. All data are presented as the mean ± SEM (n = 3), and t-tests were performed to evaluate statistical significance: ***P < 0.001 and ****P < 0.0001.

the number of neurons were observed even though no specific disease was induced. Furthermore, some pyramidal cells exhibited vesicular nuclei, and most neurons became shrunken with vacuolated cytoplasm and pyknotic nuclei in the aged WT mice (thick arrows in Fig. 3G). An increase in the population of glial cells within the molecular layer was noted in 12-month-old WT mice (arrowheads). Additionally, we verified that while these brain damage and deformation of various neuronal or glial cells were evident in all the aged mice, the extent of it was significantly lower in GIP-TG mice.

Given the findings of the *in vitro* experiments focusing on lipid peroxidation, we assessed the degree of ferroptosis in the brain tissue of 1-year-old mice through 4-hydroxynonenal (HNE) staining. The prevalent, highly toxic, stable end product of lipid peroxidation has been implicated in tissue damage, dysfunction, injury associated with aging, and other pathological conditions (20, 21). The intensity of 4-HNE staining, observed via immunofluorescence, was found to be significantly higher in aged WT mice, while it was scarcely observed in GIP-TG mice (Fig. 3H, I). These *in vivo* experiments proved that overexpression of GIP greatly inhibits the occurrence of the ferroptosis associated with aging, so we examined the expression of ferroptosis marker genes in WT and GIP-TG mice. The relative mRNA levels (Fig. 3J-M) and protein expression (Fig. 3N) of the negative ferroptosis regulators xCT/SLC7A11, glutathione peroxidase 4 (GPX4), and nuclear factor erythroid-2-related factor 2 (Nrf2) increased markedly in GIP-TG mice, while NOX1 for a ferroptosis inducer, levels decreased. In both the *in vivo* (Fig. 2) and *in vitro* (Fig. 3) experiments, GIP inhibited or delayed the ferroptosis associated with aging, which results from lipid peroxidation and fluctuations in the relevant proteins.

GIP maintains neuronal homeostasis during aging through the Epac-Rap1b signaling pathway

In previous research, GIP has been shown to mediate several physiological cAMP signal actions involving crosstalk between PKA and MAPK that are important for neuronal development and survival (22). Because of this, we deliberately chose to investigate the intricate relationship between GIP and Epac, focusing on their interactions within the cAMP downstream signaling pathway. Beginning with an investigation into mRNA levels using qRT-PCR in NB41A3 cells overexpressing GIP *in vitro*, our findings unveiled a notable increase in Epac expression (Fig. 4A). Although we observed a slight uptick in Rap1a levels, the change was not statistically significant (Fig. 4B). Therefore, we focused on other monomeric G-proteins, particularly Rap1b (23), which exhibited a clear and statistically considerable expression increase (Fig. 4C). Subsequently, western blot analyses revealed discernible increased expression of both Epac and Rap1b in GIP overexpressing cells (Fig. 4D). To clarify GIP-Epac-Rap1 signaling pathway for ferroptosis inhibition for the first time, we used the CE3F4 as an Epac1 inhibitor. We discovered that the reduction in cell number and increased cell death in the GIP overexpressing cell line was more pronounced with Epac inhibitor treatment compared to the mock group. And glutamate treatment in the presence of an Epac inhibitor significantly exacerbated glutamate-induced cell death in GIP overexpressing cell lines, markedly reducing cell viability. Additionally, when cell recovery was assessed with Ferrostatin-1 (Fer-1), a well-known ferroptosis inhibitor, there was a substantial increase in cell viability and recovery in the GIP overexpressing cell line compared to the mock cells (Fig. 4E, F). Furthermore, *in vivo* immunofluorescence experiments using cerebellum tissue of both WT and GIP-TG mice showed the co-localization of Epac and GIP (Fig. 4G). Notably, a distinct increase in Epac and Rap1b levels in GIP-TG was observed (Fig. 4H). Combining the co-localization and protein expression data of these related markers, the activation of signal transduction between GIP and Epac was successfully demonstrated. Additionally, Rap1b, a downstream signaling factor of Epac, was shown to be activated in the cerebral cortex of WT and GIP-TG mice, confirming once again through immunohistochemistry that GIP protects against oxidation by activating the Epac–Rap1b signaling pathway (Fig. 4I). In summary, we investigated the Epac-Rap1 signaling cascade both in neuronal cells and mice by specifically augmenting GIP expression in neurons showing that GIP at least delays age-related brain damage and injury occurring from ferroptosis.

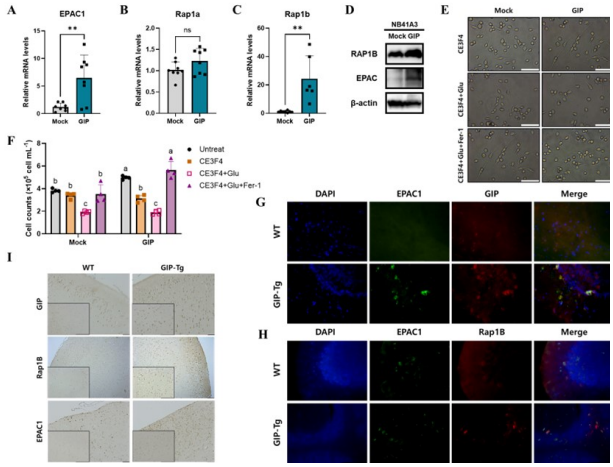

Fig. 4. Activation of the Epac–Rap1b signaling pathway by GIP alleviates brain damage. Relative mRNA levels of Epac (A), Rap1a (B), and Rap1b (C) in mock and GIP-overexpressing NB41A3 cells were determined using qPCR. (D) The protein expressions of Epac and Rap1b, as detected by western blotting. (E, F) Bright-field images and its quantification in the treatment of CE3F4, glutamate, and Ferrostain-1. (G, H) Mice sagittal sections from the cerebellum of 1-year-old mice were immunofluorescence stained for GIP (red), Epac1 (green), and DAPI (blue). (I) Coronal sections showing Epac and Rap1b staining, showing notable signal increases in the TG mice (scale bars represent 100 μm). Data are presented as means ± SEM from more than three independent experiments, and t-tests were performed to assess statistical significance: $^{**}P < 0.01$.

DISCUSSION

Although extensive research is needed to prove the associations between lipid peroxidation and aging, recent studies suggest that oxygen-derived free radicals and membrane lipid modifications are probably critical factors in the aging process. These age-associated pathologies are related to changes in cellular components and metabolism homeostasis and are also inevitable in the central nervous system. We may have also elucidated a positive correlation between aging and lipid peroxidation, as evidenced by the extent of lipid peroxidation observed in younger and older mice.

This study expanded on our previous research investigating the impact of GIP overexpression in HT-22 cells (16), broadening the range to encompass neuronal cell lines beyond hippocampal cells. As seen in HT-22 cells, upon overexpression of GIP in NB41A3 cells, we observed a smoother transition to the S and G2/M phases. The FACS data showing a decrease in the observed cell ratio of G0/G1 phase cells may imply GIP decreases cell death. Furthermore, for the first time *in vivo*, established neuron-specific GIP-TG mice showed reduced oxidative stress and the maintenance of homeostasis without damage or induction. Consequently, we opted for an aging model instead of artificial ferroptosis inducer injections to observe the protective effect of GIP *in vivo*.

Our findings also revealed that GIP triggers the activation of the Epac/Rap1b signaling pathway (Fig. 4), thereby protecting neuronal cells from ferroptosis-induced damage. It is known that Epac/Rap1b stimulation plays a crucial role in synaptic plasticity, neuronal excitability, and neuronal polarity to memory and learning (8). However, we demonstrated for the first time that aging-induced ferroptosis and possibly related chronic diseases are alleviated through GIP/Epac/Rap1 signaling using *in vitro* and *in vivo* systems. The various demonstrated effects of GIP suggest that Epac is responsible for Rap1b activation during ferroptosis inhibition and homeostasis maintenance. Also, Epac promotes the proliferation and migration of vascular smooth muscle cells and increases anti-inflammatory gene expression (24). In this regard, Fig. 3G and 4H could also be interpreted as showing enhanced blood vessels in GIP-TG mice due to the vascular endothelial cell stabilizing ability of Epac. Leveraging this insight may allow GIP to be a more effective therapeutic hormone to prevent or slow down blood vessel damage or destruction during aging while potentially expanding such therapies to other age-related diseases.

MATERIALS AND METHODS

Cell cultures and reagents

NB41A3 mouse neuroblastoma cells were maintained at 37 °C and 5% CO_2 in RPMI-1640 (Thermo Fisher Scientific, Waltham, MA, USA), and supplemented with fetal bovine serum (FBS; Gibco, Auckland, New Zealand) at 5% and streptomycin-penicillin (Gibco) at 1% and subcultured every two days.

For stimulation, the cells were seeded at a concentration of 2.0×10^5 cells/ml and incubated overnight in a 6-well culture plate (SPL Life Science, Pocheon-si, Korea) in 2 ml of RPMI. Then, the cells were treated with 100 mM glutamate (Sigma-Aldrich, St. Louis, MO, USA) in the absence or presence of ferrostatin-1 (Fer-1) (12 μM; Selleck, Shanghai, China). Another control used to investigate the downstream effects of GIP on neuronal protection was the Epac1 inhibitor (CE3F4) (20 μM; Cayman Chemical, Michigan, USA).

Establishment of GIP-overexpressing neuroblastoma cell lines

Mouse GIP was cloned into the pEGFP-N3-NSE vector and digested with HindIII and NotI. The correct sequence was then verified and amplified. NB41A3 cells (2×10^5 cells/well) were plated on six-well plates and transfected with a recombinant plasmid using Lipofectamine 2000 (Invitrogen, Carlsbad, CA, USA). Following transfection, the cells were selected by assessing their resistance to 800 μg/ml neomycin (G418) (Invitrogen, Carlsbad, CA, USA) for 2 weeks.

Generation of GIP-overexpressing mice

The neuron-specific enolase (NSE) promoter was used to generate the neuron-specific GIP overexpressing mice. Twelve-month-old C57BL/6J WT and GIP-Tg mice were housed in cages under a strict light/dark cycle. Genomic DNA was extracted from the tail, and the GIP transgene was detected via polymerase chain reaction (PCR) using GIP-specific primers. The protocols for all animal experiments followed the National Institutes of Health guidelines for the care and use of laboratory animals and were approved by the Committee for Handling and Use of Animals, Kyungpook National University.

Cell counting kit-8 (CCK-8) assay

Cell Counting Kit-8 (CCK-8; Dojindo, Kumamoto, Japan) was used to assess cell viability and proliferation. First, NB41A3 cells were seeded in 96-well plates at a density of 5,000 cells per well for 24 h. Then, glutamate was added to produce concentrations of 0-50, 80, 100, 150, and 200 mM, and the medium was seeded with NB41A3 cells and incubated for 24 h. Cell proliferation was assessed every 24 h, and relative data were calculated as a percentage of the control, which was not treated with glutamate. Cell viability and proliferation were evaluated by measuring absorbance (450 nm) using a microplate reader (BGM RABTECH, Ortenberg, Germany) after adding the CCK-8 reagent (10 μl/well).

RNA isolation and quantitative reverse transcription PCR (qRT-PCR) analysis

Cells were collected, and total cellular RNA was extracted using TRI Solution (BSK-BIO, Daegu, Korea) according to the manufacturer's instructions. Then, cDNA was synthesized with 1 μg of total RNA using the 1st Strand cDNA Synthesis Kit (TaKaRa Bio

Inc., Shiga, Japan). Real-time qPCR was performed using StepOnePlus (Applied Biosystems, Foster City, CA, USA) with SYBR Premix Ex Taq (Takara Bio Inc., Otsu, Shiga, Japan). The threshold cycle (Ct) values obtained for each reaction were normalized using the Glyceraldehyde 3-phosphate dehydrogenase (Gapdh) Ct values. All reactions were performed in triplicate.

Western blotting

Cells were lysed with lysis buffer (Thermo Fisher Scientific, Waltham, MA, USA), a 10% glycerol, 1% phosphatase, and protease inhibitor cocktail (Complete EDTA-free; Roche, Basel, Switzerland). Western blotting was performed using antibodies against anti-GIP (GTX55639; GeneTex, Irvine, CA, USA), Epac (sc-28366, 1:1,000; Santa Cruz), RAP1B (NBP1-54871, 1:1,000; Novus Biologicals), xCT/SLC7A11 (MA5-35360, Thermo Fisher Scientific), Gpx-4 (sc-166570; Santa Cruz Biotechnology, Dallas, TX, USA), nuclear factor erythroid 2-related factor (Nrf2) (sc-365949), Nox1 (ab131088; Abcam), β-actin (sc-47778), and GAPDH (#5174; Cell Signaling Technology, Danvers, MA, USA). Specific bands on the membranes were detected using the Davinch-Chemi Chemiluminescence Imaging System (CoreBio, Seoul, Korea).

Flow cytometry

For cell cycle analysis, NB41A3 cells (in a 60 mm cell culture dish) were harvested 24 after seeding, and fixed using 100% ethanol (Merck, Kenilworth, NJ, USA) at 4 ^{o}C for 1 h. Following this, the cells were washed twice with DPBS, resuspended in DPBS containing 100 μg/ml RNase A (Thermo Fisher, Waltham, MA, USA) and incubated at 37 ^{o}C for 1 h. Then, the cells were stained using 1,000 μg/ml PI (Invitrogen, Carlsbad, CA, USA) for 30 min, and fluorescence was measured with on an FACS Verse System (Becton-Dickinson, Mountain View, CA, USA).

To assess lipid peroxidation of experimental NB41A3 cell lines were either treated with 100 mM glutamate or incubated without treatment for 6 h. Then C11-BODIPY$^{581/591}$ (Thermo Fisher) was added to 2.5 μM, and the cells were incubated for 30 min.

Histologic analysis

For histologic analyses, brains from 3-month-old and 1-year-old WT and GIP-TG mice were dissected and fixed in 4% paraformaldehyde (MilliporeSigma) for 1 d after perfusion with PBS. Fixed samples were embedded in paraffin and sectioned to a thickness of 5–15 mm. The sections were then stained with H&E to evaluate the morphologic differences between the brains of WT and GIP-TG mice. Paraffin-embedded sections were used for immunofluorescent and immunohistochemistry analyses. The following antibodies were used: GIP (GTX55 639), Epac1 (sc-28366), RAP1B (NBP1-54871), 4-HNE (MA5-27570, 1:50; Thermo Fisher Scientific), anti-mouse Alexa 488 (A11001, 1:1000; Thermo Fisher Scientific), and anti-rabbit Alexa 555 (A21428, 1:1000; Thermo Fisher Scientific).

Statistical analysis

All data are presented as means ± SEM. Statistical analyses were performed using GraphPad Prism version 10 (GraphPad Software, San Diego, CA, USA), and P-values of < 0.05 were accepted as indicating statistical tests. *P < 0.05, **P < 0.01, ***P < 0.001, and ****P < 0.0001.

ACKNOWLEDGEMENTS

This research was supported by Global - Learning & Academic research institution for Master's·PhD students, and Postdocs (LAMP) Program of the National Research Foundation of Korea (NRF) grant funded by the Ministry of Education (No. RS-2023-00301914).

CONFLICTS OF INTEREST

The authors have no conflicting interests.

REFERENCES

1. Fu Y, Kaneko K, Lin HY et al (2020) Gut hormone GIP induces inflammation and insulin resistance in the hypothalamus. Endocrinology 161, 1-12
2. Ji C, Xue GF, Li G, Li D and Holscher C (2016) Neuroprotective effects of glucose-dependent insulinotropic polypeptide in Alzheimer's disease. Rev Neurosci 27, 61-70
3. Conrad M, Kagan VE, Bayir H et al (2018) Regulation of lipid peroxidation and ferroptosis in diverse species. Genes Dev 32, 602-619
4. Nguyen CTN, Kim SM and Kang YP (2022) Mass spectrometry-based approaches to explore metabolism regulating ferroptosis. BMB Rep 55, 413-416
5. Pratico D (2002) Lipid peroxidation and the aging process. Sci Aging Knowledge Environ 2002, re5
6. Jiang X and Nardelli J (2016) Cellular and molecular introduction to brain development. Neurobiol Dis 92, 3-17
7. Ster J, De Bock F, Guerineau NC et al (2007) Exchange protein activated by cAMP (Epac) mediates cAMP activation of p38 MAPK and modulation of Ca2+-dependent K+ channels in cerebellar neurons. Proc Natl Acad Sci U S A 104, 2519-2524
8. Munoz-Llancao P, Henriquez DR, Wilson C et al (2015) Exchange protein directly activated by cAMP (Epac) regulates neuronal polarization through rap1B. J Neurosci 35, 11315-11329
9. Carpenter LC, Perez-Verdugo F and Banerjee S (2024) Mechanical control of cell proliferation patterns in growing epithelial monolayers. Biophys J 123, 909-919
10. Lei L, Lu Q, Ma G, Li T, Deng J and Li W (2022) P53 protein and the diseases in central nervous system. Front Genet 13, 1051395
11. Li YQ and Wong CS (2018) Effects of p21 on adult hippocampal neuronal development after irradiation. Cell Death Discov 4, 15
12. Macleod KF, Sherry N, Hannon G et al (1995) p53-dependent and independent expression of p21 during cell growth, differentiation, and DNA damage. Genes Dev 9, 935-944
13. Lee E, Song CH, Bae SJ, Ha KT and Karki R (2023) Regulated cell death pathways and their roles in homeostasis,

infection, inflammation, and tumorigenesis. Exp Mol Med 55, 1632-1643
14. Ankarcrona M, Dypbukt JM, Bonfoco E et al (1995) Glutamate-induced neuronal death: a succession of necrosis or apoptosis depending on mitochondrial function. Neuron 15, 961-973
15. Drummen GP, Gadella BM, Post JA and Brouwers JF (2004) Mass spectrometric characterization of the oxidation of the fluorescent lipid peroxidation reporter molecule C11-BODIPY(581/591). Free Radic Biol Med 36, 1635-1644
16. Ko J, Jang S, Kwon W et al (2022) Protective effect of GIP against monosodium glutamate-induced ferroptosis in mouse hippocampal HT-22 cells through the MAPK signaling pathway. Antioxidants (Basel) 11, 189
17. Kim YJ and Hyun J (2023) Mechanosensitive ion channels in apoptosis and ferroptosis: focusing on the role of Piezo1. BMB Rep 56, 145-152
18. Qin K, Zhang F, Wang H et al (2023) circRNA circSnx12 confers Cisplatin chemoresistance to ovarian cancer by inhibiting ferroptosis through a miR-194-5p/SLC7A11 axis. BMB Rep 56, 184-189
19. Cho YM and Kieffer TJ (2010) K-cells and glucose-dependent insulinotropic polypeptide in health and disease. Vitam Horm 84, 111-150
20. Shoeb M, Ansari NH, Srivastava SK and Ramana KV (2014) 4-Hydroxynonenal in the pathogenesis and progression of human diseases. Curr Med Chem 21, 230-237
21. Zhang H and Forman HJ (2017) 4-hydroxynonenal-mediated signaling and aging. Free Radic Biol Med 111, 219-225
22. Harada N and Inagaki N (2017) Role of GIP receptor signaling in beta-cell survival. Diabetol Int 8, 137-138
23. Mitra RS, Zhang Z, Henson BS, Kurnit DM, Carey TE and D'Silva NJ (2003) Rap1A and rap1B ras-family proteins are prominently expressed in the nucleus of squamous carcinomas: nuclear translocation of GTP-bound active form. Oncogene 22, 6243-6256
24. Parnell E, Palmer TM and Yarwood SJ (2015) The future of Epac-targeted therapies: agonism versus antagonism. Trends Pharmacol Sci 36, 203-214